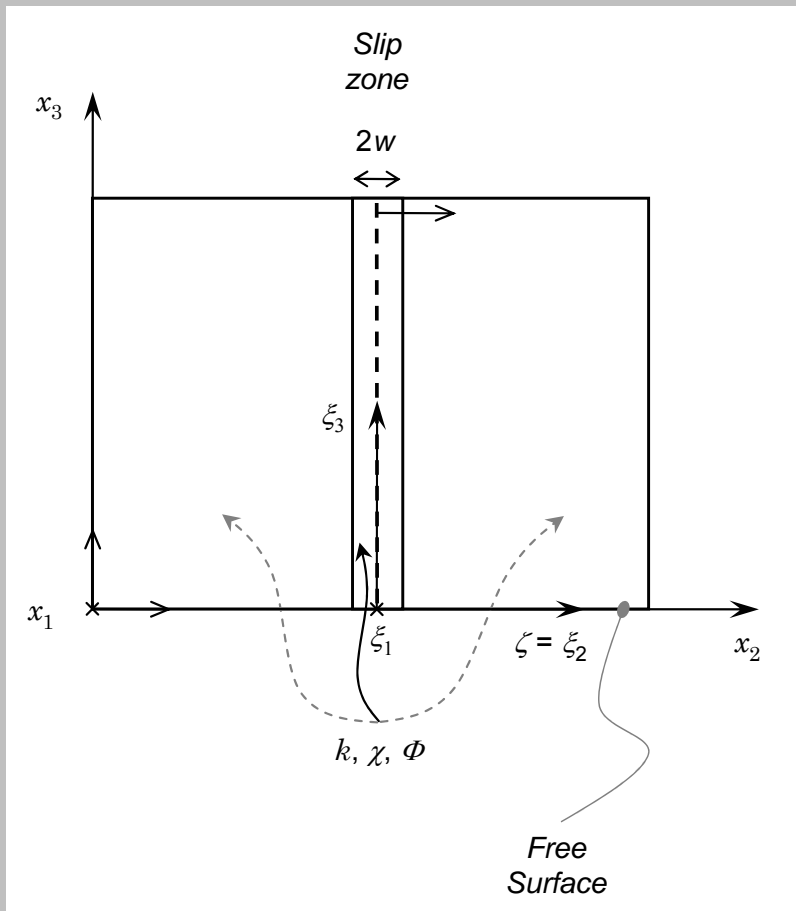


An aerial photograph of a geothermal field, likely in Iceland. The landscape is a mix of dark, wet mud and light-colored, mineral-rich soil. Numerous small, white plumes of steam or gas are visible rising from the ground across the field. The terrain appears rugged and somewhat barren, typical of a high-temperature geothermal environment.

**Application I. Thermal
pressurization of pore fluids**

Mathematical background



1 – D Fourier' s heat conduction equation:

$$\frac{\partial}{\partial t} T = \chi \frac{\partial^2}{\partial \zeta^2} T + \frac{1}{c} q$$

Coupling of temperature T with pore fluid pressure p_{fluid} :

$$\frac{\partial}{\partial t} p_{fluid} = \frac{\alpha_{fluid}}{\beta_{fluid}} \frac{\partial}{\partial t} T - \frac{1}{\beta_{fluid} \Phi} \frac{\partial}{\partial t} \Phi + \omega \frac{\partial^2}{\partial \zeta^2} p_{fluid}$$

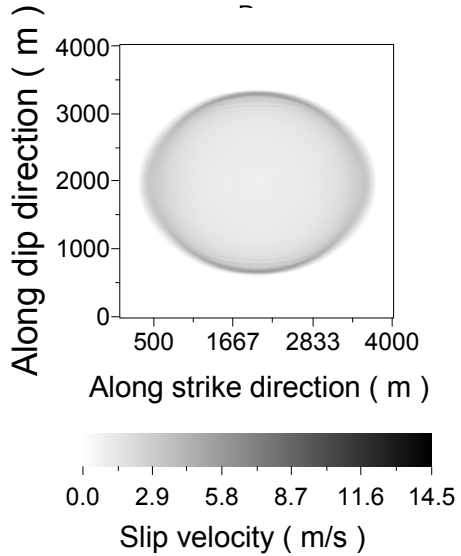
where χ is the thermal diffusivity, c the heat capacity for unit volume, α_{fluid} the coefficient of thermal expansion, β_{fluid} the compressibility coefficient, Φ the porosity and $\omega = k/\eta_{fluid} \beta_{fluid} \Phi$ the hydraulic diffusivity (being k the permeability of the medium and η_{fluid} the dynamic fluid viscosity). Analytical solutions at $\zeta = 0$ are:

$$T^{wf}(\xi_1, \xi_3, t) = T_0^f + \frac{1}{2cw(\xi_1, \xi_3)} \int_0^{t-\varepsilon} dt' \operatorname{erf}\left(\frac{w(\xi_1, \xi_3)}{2\sqrt{\chi(t-t')}}\right) \tau(\xi_1, \xi_3, t') v(\xi_1, \xi_3, t')$$

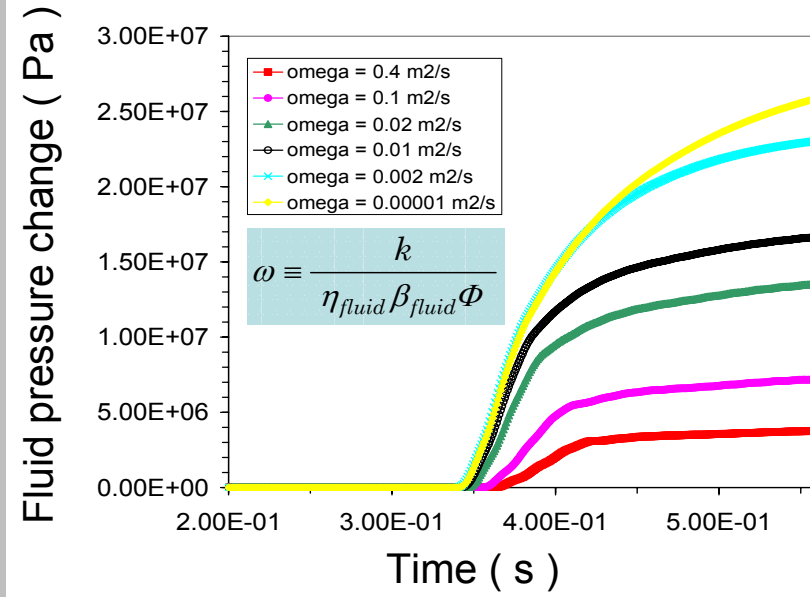
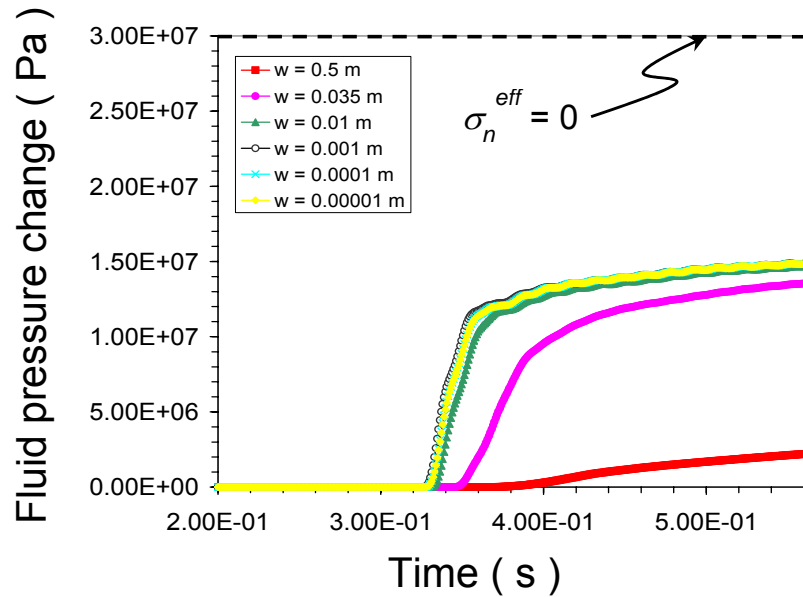
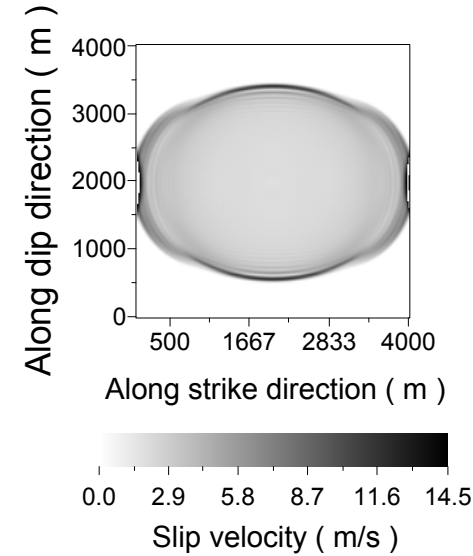
$$\begin{aligned} \tilde{p}_{fluid}^{wf}(\xi_1, \xi_3, t) = & p_{fluid_0}^f + \frac{\gamma}{2w(\xi_1, \xi_3)} \int_0^{t-\varepsilon} dt' \left\{ -\frac{\chi}{\omega - \chi} \operatorname{erf}\left(\frac{w(\xi_1, \xi_3)}{2\sqrt{\chi(t-t')}}\right) + \frac{\omega}{\omega - \chi} \operatorname{erf}\left(\frac{w(\xi_1, \xi_3)}{2\sqrt{\omega(t-t')}}\right) \right\} \\ & \left\{ \tau(\xi_1, \xi_3, t') v(\xi_1, \xi_3, t') - \frac{2w(\xi_1, \xi_3)}{\gamma} \frac{1}{\beta_{fluid} \Phi(t')} \frac{\partial}{\partial t'} \Phi(\xi_1, 0, \xi_3, t') \right\} \end{aligned}$$

Results with SW law

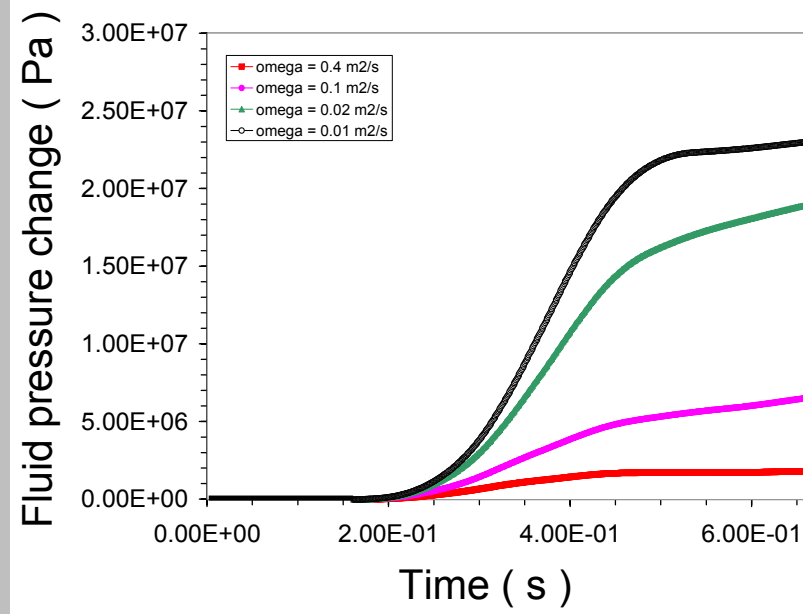
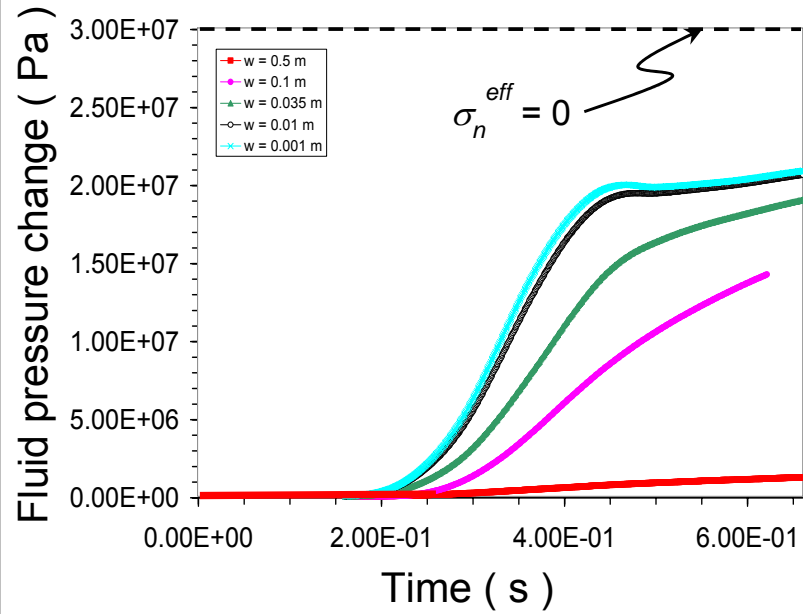
Dry fault ($\sigma_n^{eff} = \text{const}$)



Wet fault (σ_n^{eff} varies)

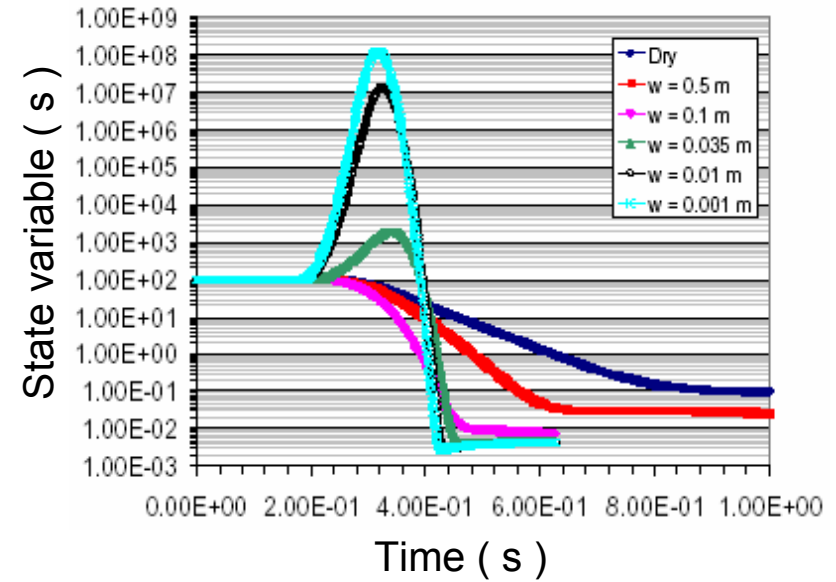
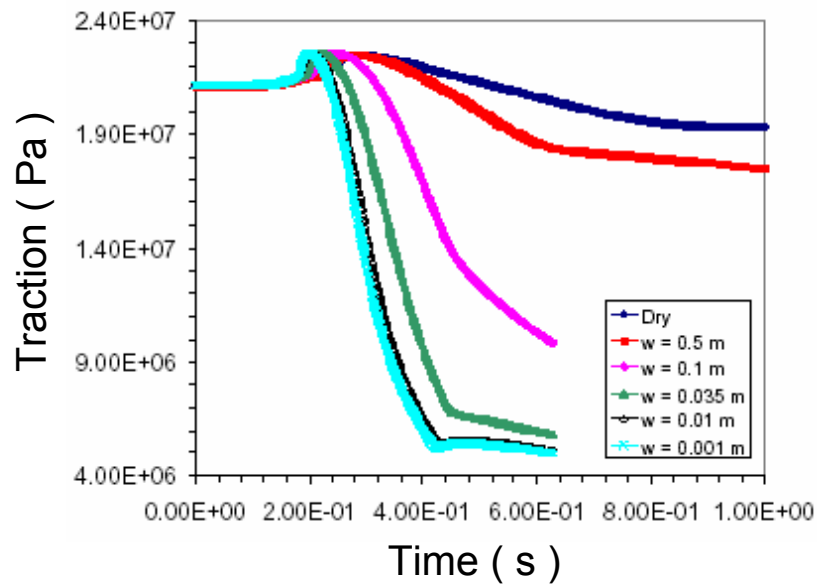
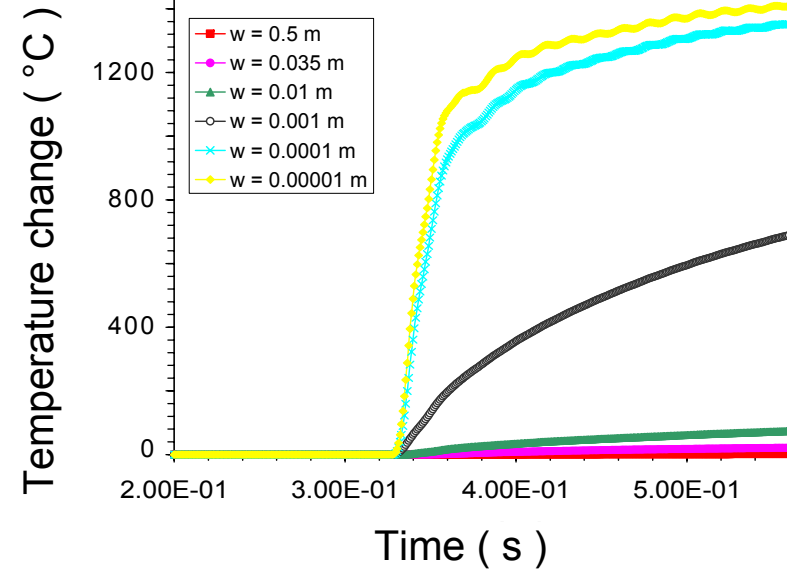
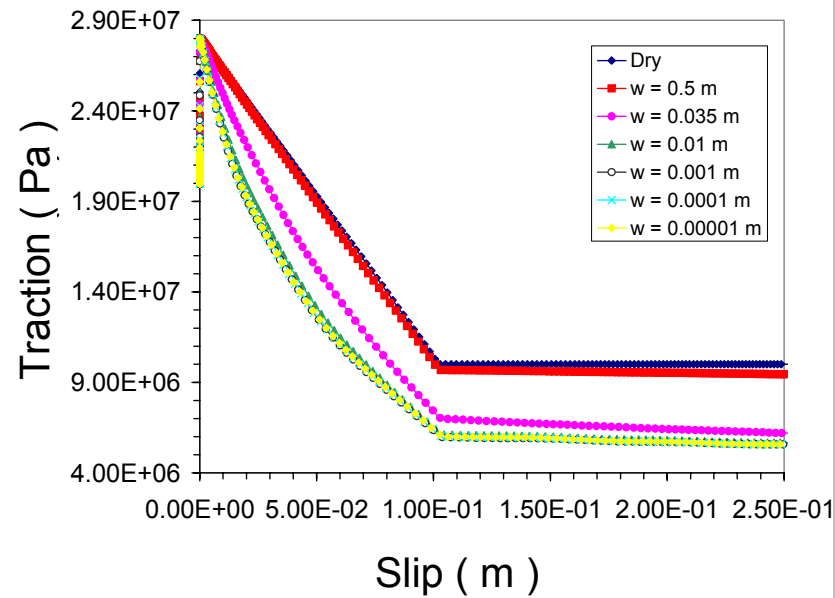


Results with DR law





The breakdown zone



An aerial photograph of a wet, muddy landscape, possibly a floodplain or a large-scale construction site. The ground is a mix of light brown and grey mud, with several large, dark, irregularly shaped areas that appear to be pools of water or very saturated mud. The overall scene is desaturated and has a grainy texture. A semi-transparent grey rectangular box is overlaid in the center of the image, containing the text.

**Application II. Flash heating
of micro – asperity contacts**

Mathematical background

RUINA – DIETERICH WITH FLASH HEATING

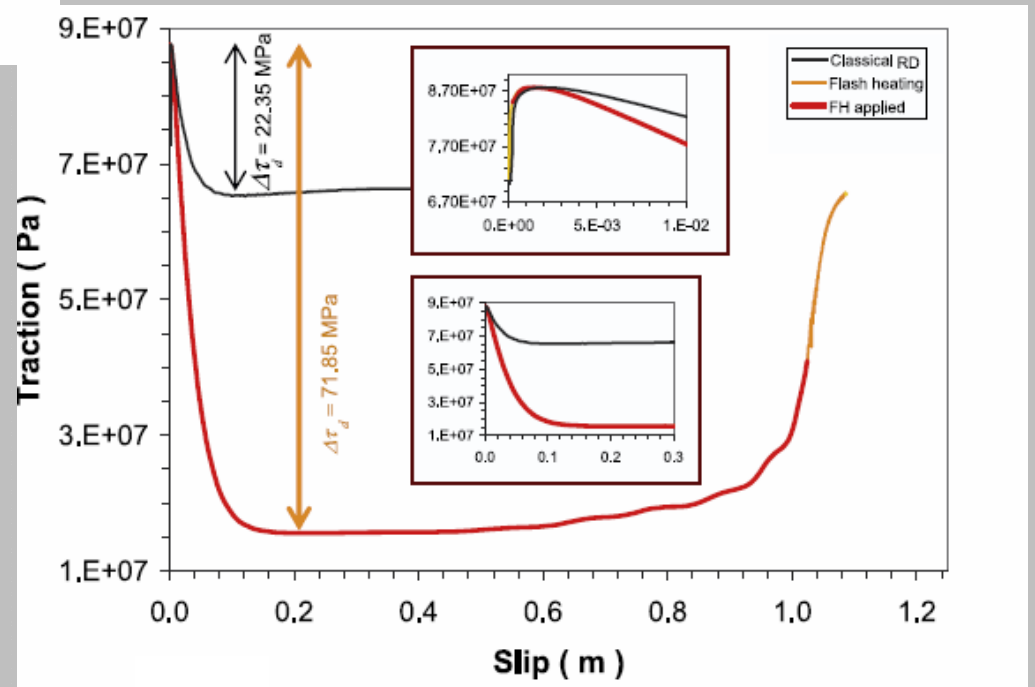
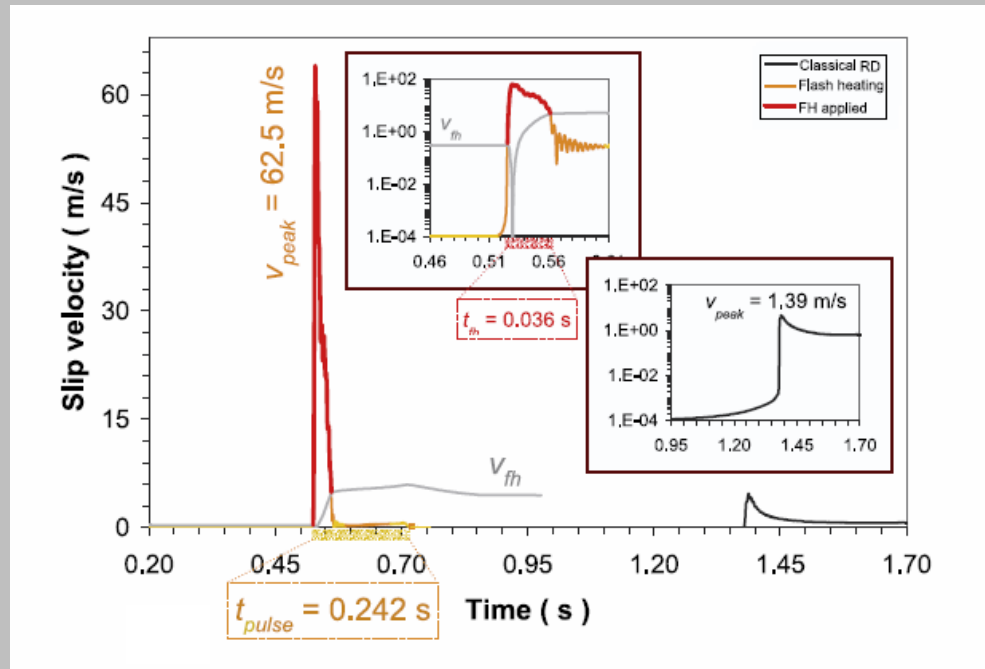
$$\left\{ \begin{array}{l} \tau = \left[\mu_* - a \ln \left(\frac{v_*}{v} \right) + \theta \right] \sigma_n^{eff} \\ \frac{d}{dt} \theta = \begin{cases} -\frac{v}{L} \left[\theta + b \ln \left(\frac{v}{v_*} \right) \right] & , v \leq v_{fh} \\ -\frac{v}{L} \left[\theta + b \frac{v_{fh}}{v} \ln \left(\frac{v}{v_*} \right) + \left(1 - \frac{v_{fh}}{v} \right) \left(a \ln \left(\frac{v}{v_*} \right) + \mu_* - \mu_{fh} \right) \right] & , v > v_{fh} \end{cases} \end{array} \right.$$

where $v_{fh} = \frac{\pi\chi}{D_{ac}} \left(c \frac{T_{weak} - T^{wf}}{\tau_{ac}} \right)^2$ is

a weakening velocity above which flash heating is activated, T_{weak} is a weakening temperature, τ_{ac} is the (average) shear strength of asperity contacts and D_{ac} their (average) size.

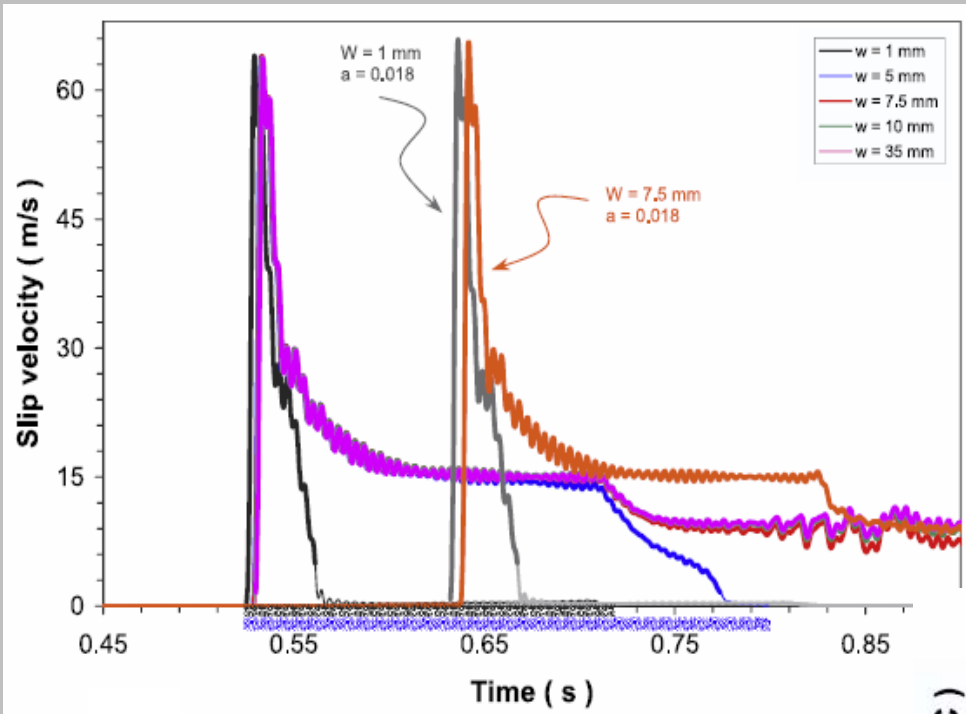


Crack - like ruptures or slip pulses?

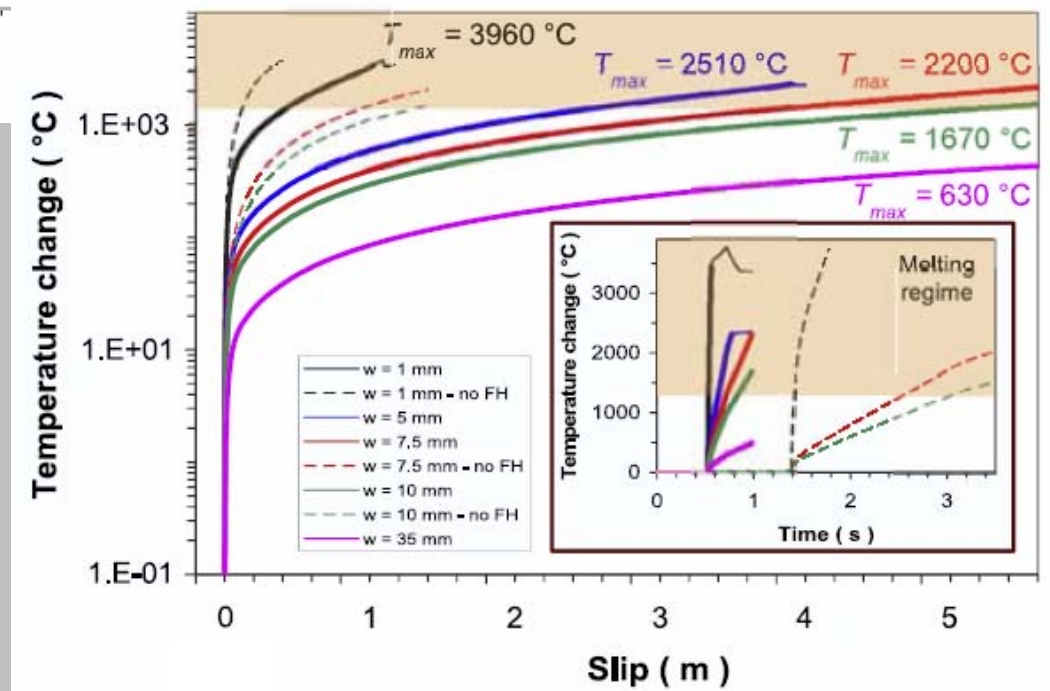




The prominent importance of $2w$



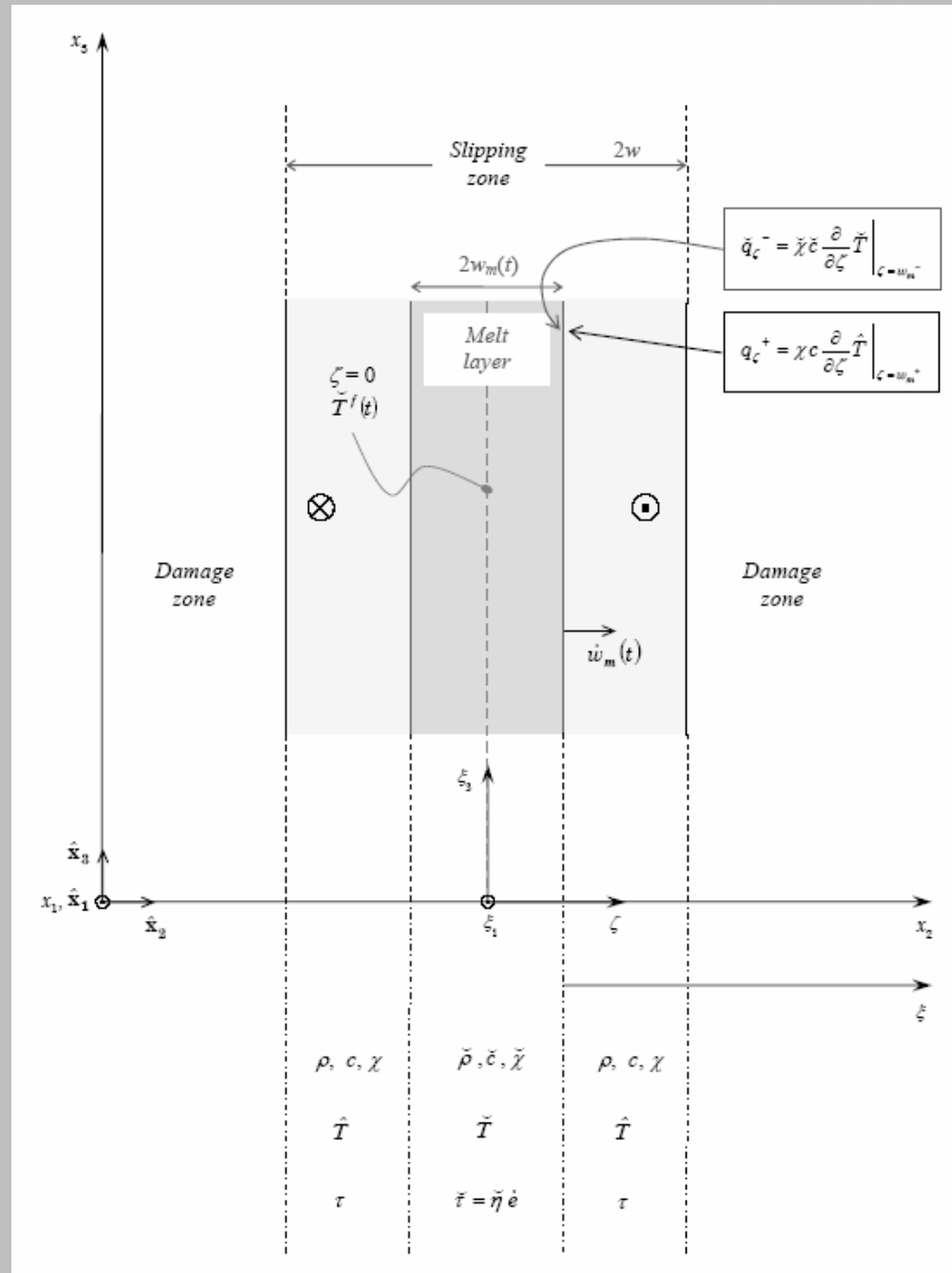
Localized shear ($2w \leq 10$ mm):
self-healing pulses



An aerial photograph showing a large, dark, irregularly shaped area on a light-colored, textured ground surface. The dark area appears to be a melt pond or a gouge, possibly formed by the melting of rocks. The surrounding ground is light-colored and has a rough, granular texture. The dark area is roughly rectangular but has jagged edges and some internal features. The overall scene is a wide, flat expanse of ground with a prominent dark feature in the center.

**Application III. Melting of
rocks and gouge**

Mathematical background



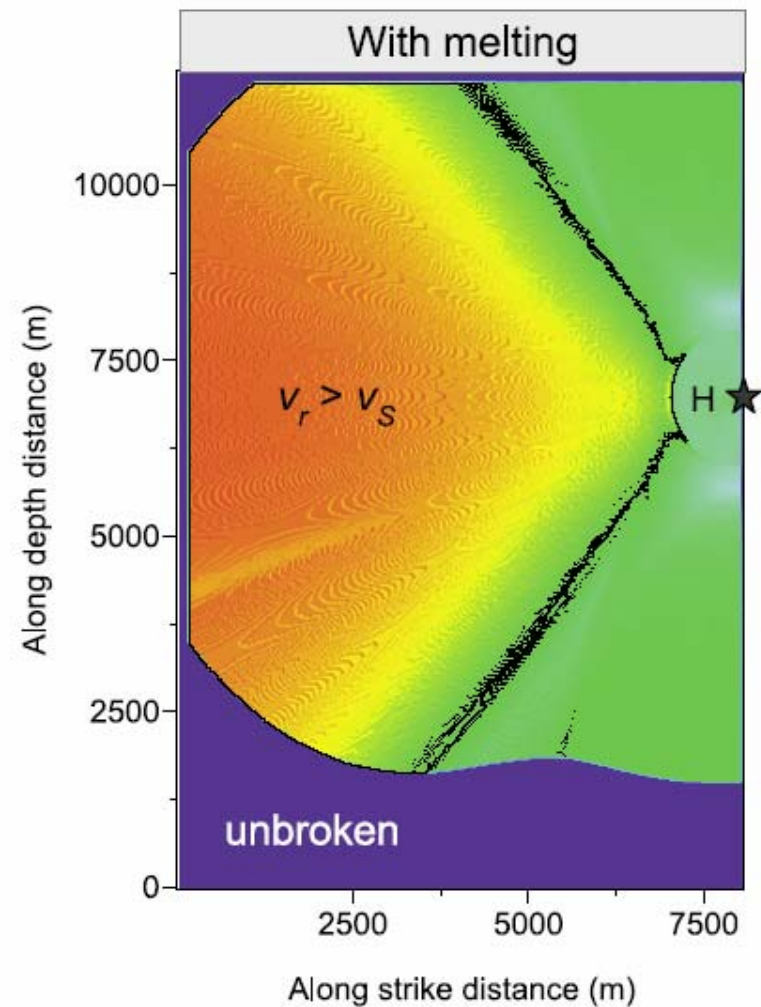
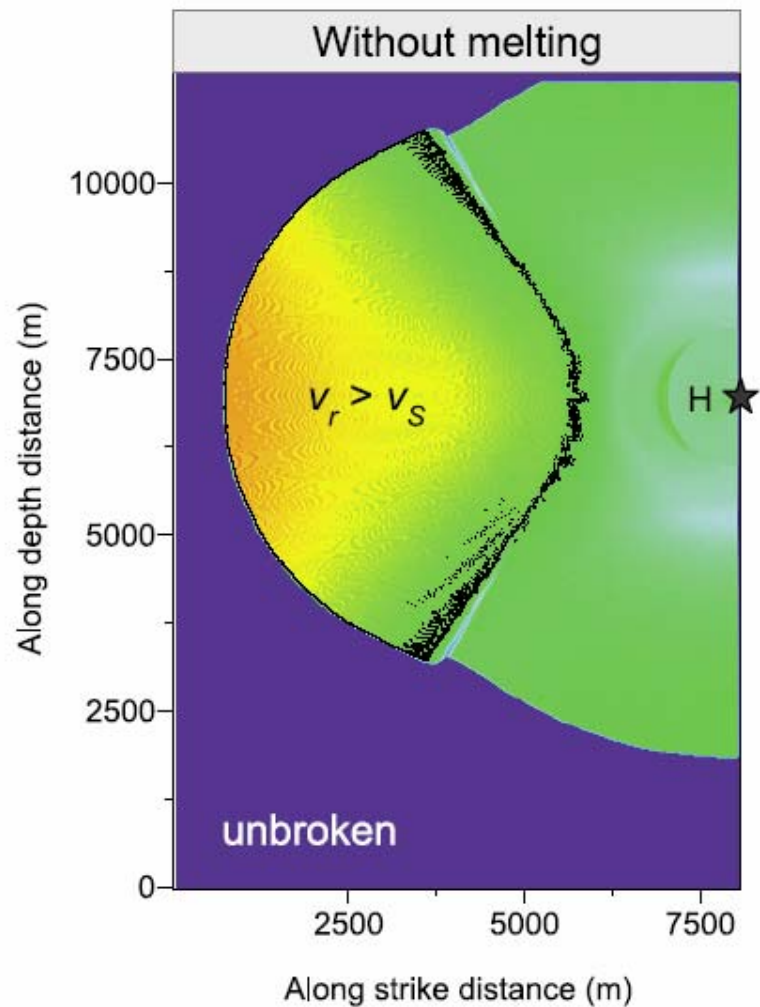
Mathematical background

Coulomb friction is no longer valid and we then consider a Newtonian fluid (e.g., Fialko, 2004):

$$\tau^{(\text{NF})} = \tilde{\eta} \frac{v}{2w_m}$$

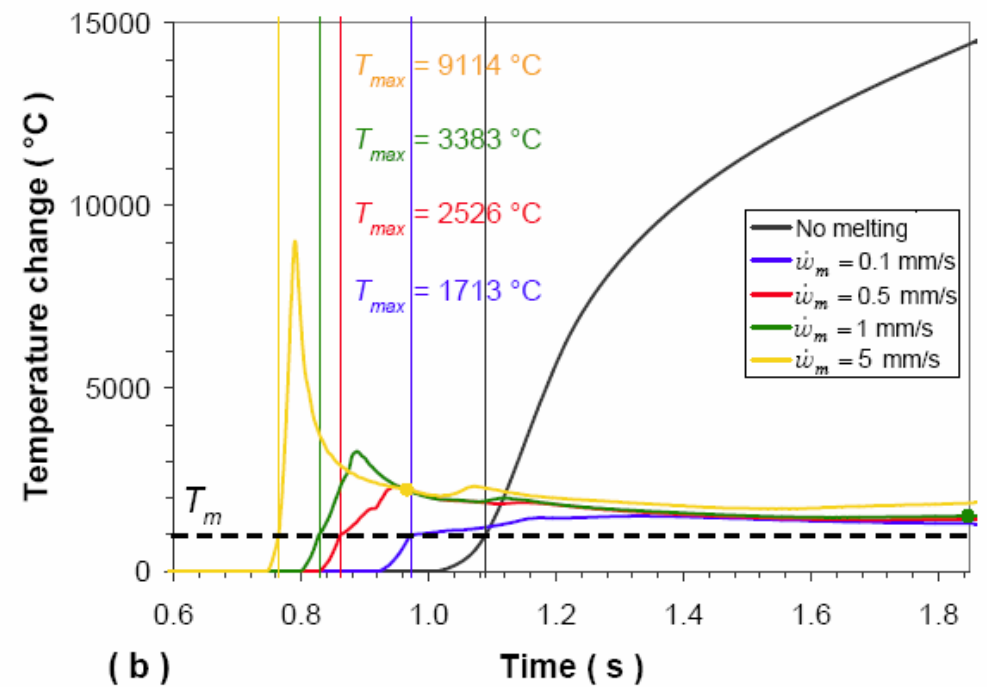
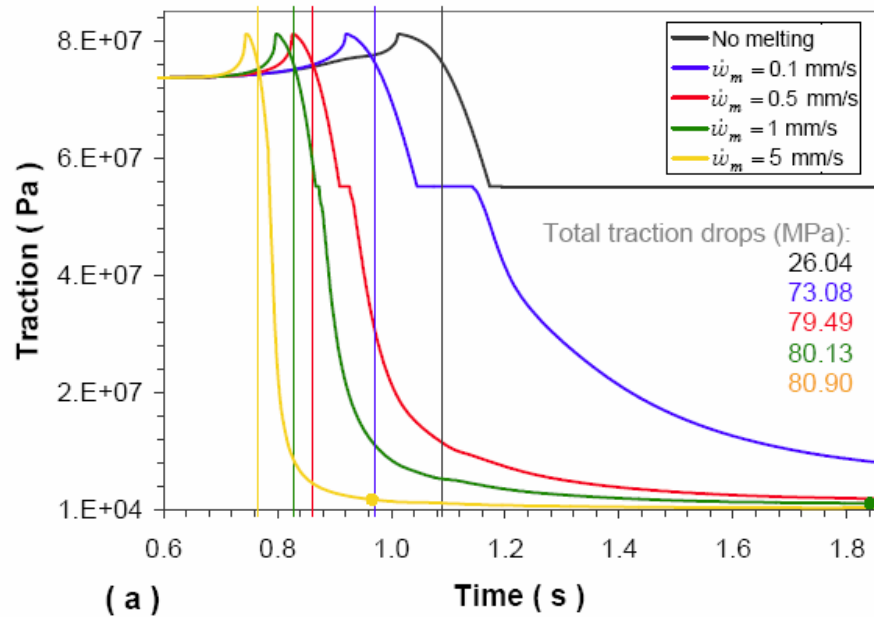
$$\tilde{\eta}(\zeta, t) = \tilde{K} e^{\frac{\tilde{T}_a}{T(\zeta, t-\varepsilon) + 273.15}}$$


Melting enhances supershear EQs





Transition to a viscous rheology

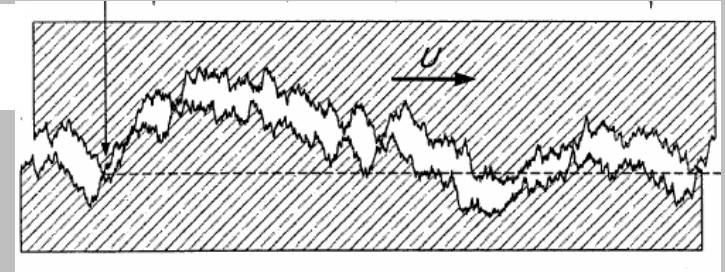




**Application IV. Mechanical
Lubrication**

Mathematical background

Brodsky and Kanamori (2001)



$$\tau = \begin{cases} \mu_u \sigma_n^{\text{eff}} + \frac{\langle 2w \rangle}{u} p_{\text{lub}} = \mu_u \sigma_{n_0} - \left(\mu_u - \frac{\langle 2w \rangle}{u} \right) p_{\text{lub}} & , So < 1 \\ \frac{\langle 2w \rangle}{u} p_{\text{lub}} & , So \geq 1 \end{cases}$$

Effective normal stress $\sigma_n^{\text{eff}} = \sigma_n - p_{\text{res}} - p_{\text{lub}}$

Sommerfeld number $So \equiv \frac{p_{\text{res}} + p_{\text{lub}}}{\sigma_n}$

$$\langle 2w \rangle^3 p_{\text{lub}} - 6\eta r u^2 v = 0$$

In the special case of (temporally) constant gap height ($\langle 2w \rangle = \langle 2w_0 \rangle$)

Lubrication pressure

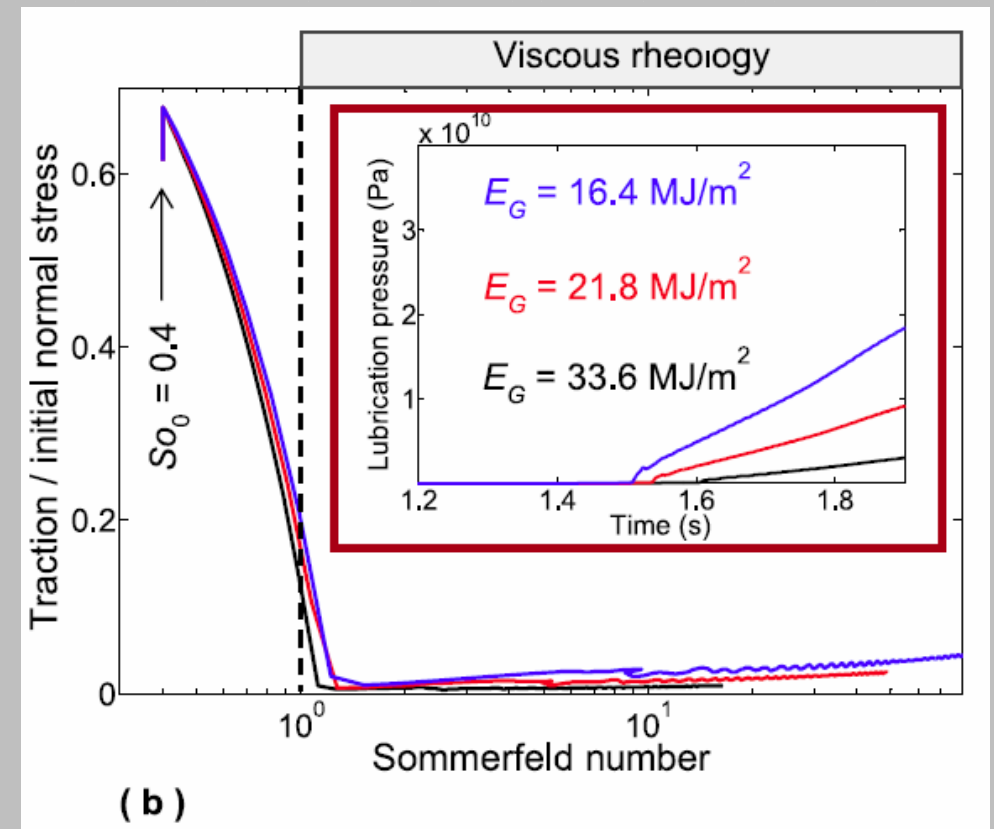
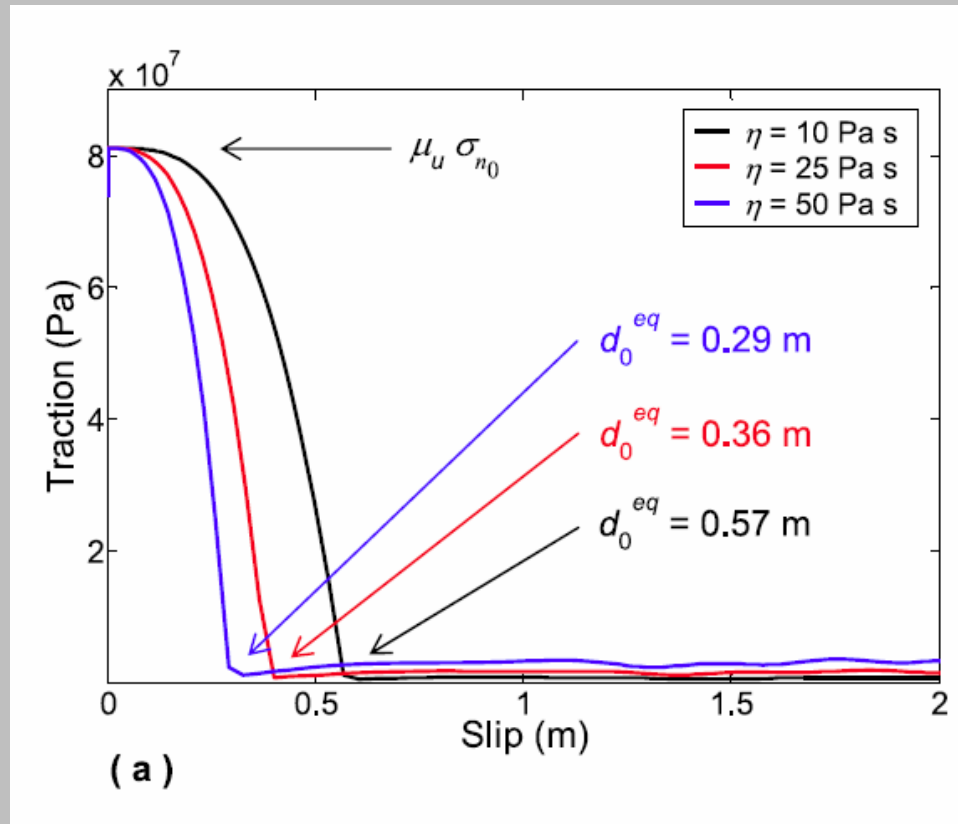
$$\frac{6\eta r}{\langle 2w_0 \rangle^3} u^2 v$$

Frictional resistance

$$\begin{cases} \mu_u \sigma_{n_0} - \frac{6\eta r \mu_u}{\langle 2w_0 \rangle^3} u^2 v + \frac{6\eta r}{\langle 2w_0 \rangle^2} u v & , So < 1 \\ \frac{6\eta r}{\langle 2w_0 \rangle^2} u v & , So \geq 1 \end{cases}$$

Bizzarri (2012, *JGR*, **117**, B05304)

Viscous rheology after $So = 1$



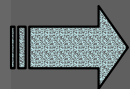
Conclusions

- ✓ Many different physical and chemical mechanisms may occur during faulting
- ✓ They strongly affect the overall dynamics of the fault, the radiated energy and the resulting ground motions
- ✓ Thermal pressurization of pore fluids, flash heating, melting and mechanical lubrication tend to enhance supershear ruptures...
- ✓ ... produce a nearly complete stress drop (heat paradox)
- ✓ ... increase the (equivalent) slip–weakening distance and thus the “fracture” energy
- ✓ In some cases the weakening behavior becomes exponential, as suggested by laboratory observations

- ✓ Different competing mechanisms can significantly affect the recurrence time of an earthquake sequence...
- ✓ ... and they can make the concept itself of the seismic cycle meaningless

Open questions and future developments

- 1) Theoretical results will predict a nearly complete stress drop and therefore we should find a signature of these high stress drop values in the recorded seismograms. Seismological estimates of stress drop do not support such an evidence;



the estimation of stress drop from seismic waves is biased (for instance by the difficulties in analyzing high frequency radiation)

or

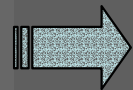
the effects of pressurization, melting and so on on the dynamic traction evolution are less pronounced

2) We need to test theoretical predictions against laboratory evidence; numerical results definitively represent an input for the development of next-generation machines

⇒ Current high velocity lab. experiments only deal with friction (of pre-cut surfaces) and not with fracture (of intact rocks)

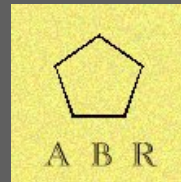
⇒ We need to reproduce real-world conditions in terms of BOTH high sliding velocity and confining stress

3) Do real data (recorded during natural earthquakes) contain signatures of the specific friction law governing the seismicogenic fault?



We know from numerical models that, for ruptures having exactly the same energetics (namely, the same fracture energy density), the resulting ground motions are virtually indistinguishable

This slide is empty intentionally.



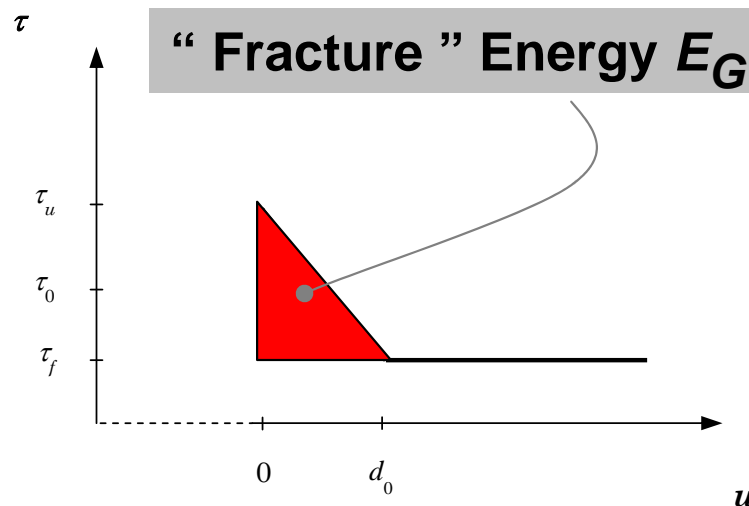
Support Slides: Parameters, Notes, etc.

To not be displayed directly. Referenced above.

Slip - Weakening Friction Laws



$$\tau = \begin{cases} \left[\mu_u - (\mu_u - \mu_f) \frac{u}{d_0} \right] \sigma_n^{eff} & , u < d_0 \\ \mu_f \sigma_n^{eff} & , u \geq d_0 \end{cases}$$



Barenblatt (1959a, 1959b), Ida (1972), Andrews (1976a, 1976b), and many authors thereafter

d_0 is the characteristic slip –
weakening distance

Rate - and State - Dependent

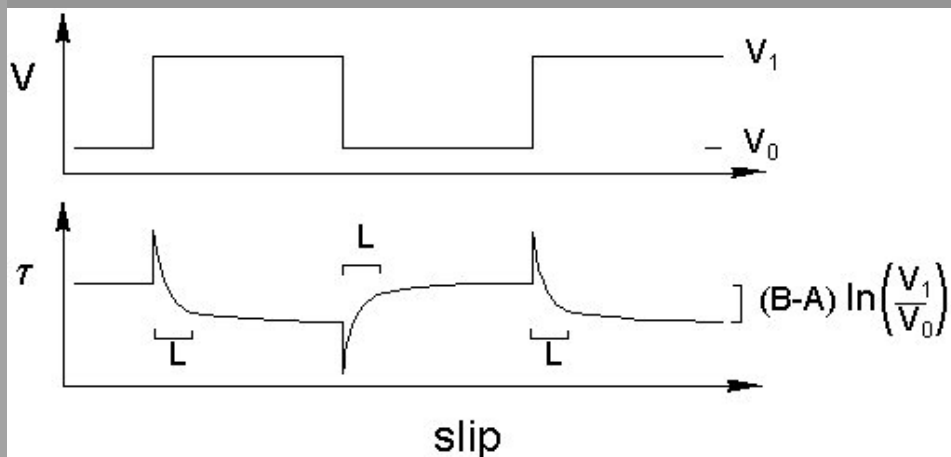


DIETERICH – RUINA WITH VARYING NORMAL STR.

$$\left\{ \begin{array}{l} \tau = \left[\mu_* - a \ln \left(\frac{v_*}{v} \right) + b \ln \left(\frac{\Psi v_*}{L} \right) \right] \sigma_n^{eff} \\ \frac{d}{dt} \Psi = 1 - \frac{\Psi v}{L} - \left(\frac{\alpha_{LD} \Psi}{b \sigma_n^{eff}} \right) \frac{d}{dt} \sigma_n^{eff} \end{array} \right.$$

Linker and Dieterich (1992), Dieterich and Linker (1992), Bizzarri and Cocco (2006a, 2006b)

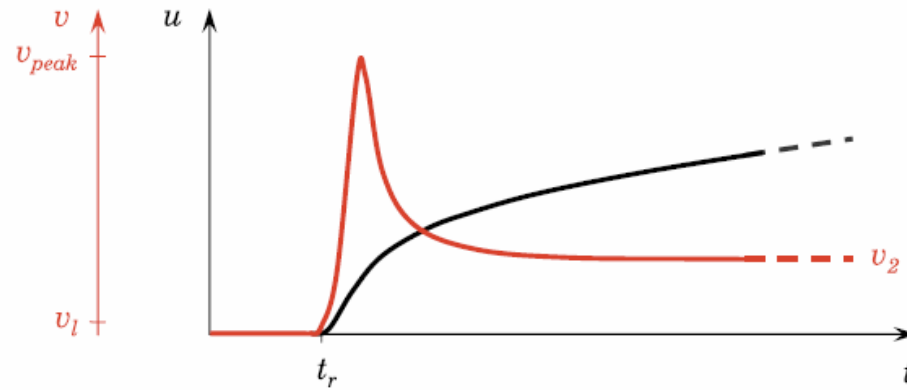
Response to an abrupt jump in load



Crack vs. Pulse

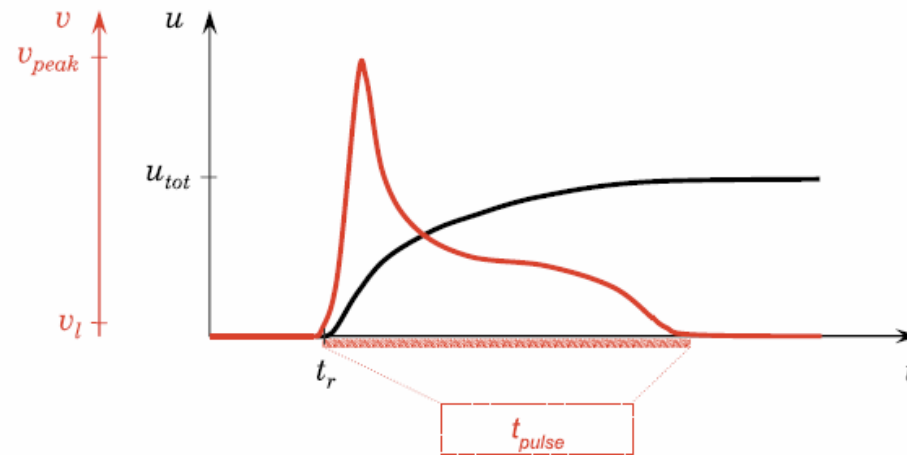


Crack-like rupture



(a)

Pulse-like rupture



(b)